Vortex dynamics and critical current in superconductors with unidirectional twin boundaries

Hidehiro Asai* and Satoshi Watanabe
Department of Materials Engineering, The University of Tokyo, 7-3-1 Hongo, Bunkyo-ku, Tokyo 113-8656, Japan
(Received 29 December 2007; revised manuscript received 4 May 2008; published 27 June 2008)

We have studied the dynamics of vortices interacting with unidirectional twin boundaries (TBs) in a superconductor using molecular-dynamics simulation based on the overdamped equation of vortex motion. Current-voltage curves and critical currents have been calculated as a function of vortex density. We found that the critical current as a function of vortex density reveals a staircase pattern and this pattern depends on the pinning strength. This behavior corresponds to discontinuous change of vortex configurations, which reflects vortex pinning characteristics of superconductors with TBs. We also discuss the effect of matching between vortex lattice and TBs and reveal that its behavior is different from the one in the case of columnar pinning.

DOI: 10.1103/PhysRevB.77.224514 PACS number(s): 74.25.Qt, 74.25.Sv

I. INTRODUCTION

In type-II superconductors, magnetic flux penetrates into samples in the form of vortex lines when an applied magnetic field is larger than the lower critical fields. The pinning of these vortices is important in device applications of superconductors because immobilization of vortices at pinning sites is essential for lossless transport. Therefore, considerable efforts have been made to create artificial pinning sites that can immobilize vortices effectively and increase the critical current (J_c).[1–8] With the development of various techniques to introduce artificial pinning sites, control and manipulation of vortex motion have also been studied. Recently, some groups have reported rectified motion of vortices in a sample with asymmetric pinning potential.[9,10] Furthermore, vortex dynamics interacting with various pinning centers is also an attractive subject in statistical physics. Vortices take various phases such as vortex glass[11] and Bose glass,[12] and these phase diagrams have been studied extensively.[13–15]

Correlated disorders, such as columnar defects and planar defects, are expected to be effective pinning sites since they can pin vortices in the shape of "lines." The twin boundary (TB) is one of the correlated disorders and possible candidate for tangible pinning site in the orthorhombic compound $YBa_2Cu_3O_{7-x}$ (YBCO). Thus, their pinning properties have been actively studied by both experimental and theoretical methods, and various interesting phenomena have been reported.[16–25] It has been found that the TB acts as a barrier for the vortices moving perpendicular to twin planes, while it can be easy-flow channels for vortices moving parallel to a twin plane.[16,17,19,20] Recently, it has become possible to fabricate high-density TBs in melt grown YBCO, and the pinning enhancement has been reported in the fabricated samples.[26–28] However, vortex dynamics in superconductors with high-density TBs are not clear. Although several numerical studies about the dynamics of vortices interacting with TBs have already been reported, the twin spacing T_w is much larger than the vortex spacing d in these studies. In superconductors with high-density TBs, the relation between d and T_w may affect vortex dynamics significantly. Hence numerical simulation in the case where d and T_w are comparable is favorable.

In the superconductors with periodic columnar defects, it is well known that the enhancement of pinning efficiency occurs at the magnetic fields at which the number of vortices is an integral multiple or fractional numbers of that of pinning cites.[29–31] This phenomenon comes from geometrical commensuration between the configuration of vortices and pinning sites and is called "matching effect." In the superconductors with mosaiclike TBs, matchinglike effects have also been reported when d is equal to $1/2\ T_w$ (Refs. 27 and 28) or $1/3\ T_w$.[25] Unlike columnar defects which trap only one vortex, TB can trap multiple vortices in its plane. Therefore, the matching effect between vortices and TBs is thought to be different from the one in the case of columnar defects.

Vortex dynamics interacting with TBs is analogous to two-dimensional (2D) vortex dynamics in the presence of one-dimensional (1D) pinning arrays. The physics of 2D vortices in the presence of 1D periodic pinning potential has been studied theoretically and experimentally since the 1970s,[32–36] and the matching effect has already reported. Theoretical studies have also revealed stable vortex configurations.[33–35] However, these studies considered only the region where d is larger than the wavelength of potential modulation λ_g. Therefore, vortex configurations in the region where $d<\lambda_g$ are still unclear.

In this study, we perform molecular-dynamics simulation of vortices interacting with unidirectional periodic TBs in the region where the vortex lattice constant and twin spacing are comparable. We analyze the change in vortex states and critical currents with varying vortex density. We have found a stepwise change in J_c due to the abrupt change in vortex configuration. We have also found that the stepwise change depends on pinning strength. Furthermore, J_c steps can be regarded as broad peaks coming from the effects of matching between the vortex lattice and periodic arrays of TBs.

II. MODEL AND METHOD

In our simulation, we consider a two-dimensional slice in the x-y plane of an infinite three-dimensional sample. We use periodic boundary conditions in the x-y plane and treat the vortices as stiff rods that are perpendicular to the slab surface: this implies that the applied magnetic field can be expressed as $\boldsymbol{H}=H\hat{z}$ using the unit vector in the z direction $\hat{z}$. For simplicity, we assume TBs are dominant pinning centers

and ignore all the other kinds of pinning centers. We assume TB planes are perpendicular to the x axis and align at regular intervals. The applied current is oriented in the direction of the y axis so that the Lorentz force acts perpendicular to TBs. Vortex motion is determined by solving the following overdamped equation:[20–23]

$$\eta \frac{d}{dt}\boldsymbol{r}_i = \boldsymbol{F}_{\mathrm{vv}} + \boldsymbol{F}_{\mathrm{tb}} + \boldsymbol{F}_{\mathrm{th}} + \boldsymbol{F}_L. \tag{1}$$

Here, η is the viscous coefficient which is set to unity, $\boldsymbol{r}_i$ is the location of ith vortex, $\boldsymbol{F}_{\mathrm{vv}}$ is the repulsive force from other vortices, $\boldsymbol{F}_{\mathrm{tb}}$ is the pinning force from TBs, $\boldsymbol{F}_{\mathrm{th}}$ is the thermal noise, and $\boldsymbol{F}_L$ is the Lorentz force. The form of $\boldsymbol{F}_{\mathrm{vv}}$ can be derived from the London theory as[20,37]

$$\boldsymbol{F}_{vv} = \sum_{j\neq i}^{N_v} \frac{\Phi_0^2}{8\pi^2\lambda^3} K_1\left(\frac{|\boldsymbol{r}_i - \boldsymbol{r}_j|}{\lambda}\right) \frac{\boldsymbol{r}_i - \boldsymbol{r}_j}{|\boldsymbol{r}_i - \boldsymbol{r}_j|}, \tag{2}$$

where λ is the penetration depth, Φ_0 is the flux quantum, N_V is the number of vortices, and K_1 is the modified Bessel function. Since K_1 decays quickly, we cut off this interaction force at 6 λ for computational efficiency. The TB is modeled as an attractive channel with a width of $2R_{\mathrm{tb}}$, and $\boldsymbol{F}_{\mathrm{tb}}$ is given by

$$\boldsymbol{F}_{\mathrm{tb}} = -f_{\mathrm{tb}} \sum_{k=1}^{N_{\mathrm{tb}}} x_{ik}(1 - x_{ik}^2)\Theta(1 - |x_{ik}|)\hat{x}. \tag{3}$$

Here, f_{tb} is the pinning strength of TB, N_{tb} is the number of the TBs, $x_{ik}=(\hat{x}\cdot\boldsymbol{r}_i - R_k)/R_{\mathrm{tb}}$ with R_k the x coordinate of kth TB, and Θ is the Heaviside step function. We take $R_{\mathrm{tb}}=0.15\lambda$, and twin spacing is equal to 1.2 λ. The thermal fluctuation is assumed to be a Gaussian white noise. The Lorentz force $\boldsymbol{F}_L$ is modeled as uniform force acting on all vortices. Throughout this work we take the magnetic penetration length λ as a constant parameter, and all lengths are measured in units of λ, forces in units of $f_0=\Phi_0^2/8\pi^2\lambda^3$, energies in units of $U_0=\Phi_0^2/8\pi^2\lambda^2$, vortex density in units of $B_0=\Phi_0/\lambda^2$, and time in units of $t_0=\eta\lambda/f_0$. Our system size ranges from 12 $\lambda\times$12 λ to 24 $\lambda\times$24 λ to treat various scales of vortex density. As shown in Sec. III, vortices form various lattice configurations that are commensurate with the periodic structure of TBs in several vortex density regions. We chose vortex density carefully to avoid these lattices having defects coming from the finite number of TBs.

We obtain the initial vortex position using simulated annealing method. We start from a high temperature where k_BT equals $0.01U_0$ and then reduce the temperature to zero step by step in increments of $0.0002U_0$. At each step, we keep the temperature for 1.5×10^5 MD steps. After getting a static configuration, we start to apply Lorentz force and calculate the average vortex velocity in the x direction $\hat{v}_x$ using Eq. (1) at 0 K. Note that the third term of Eq. (1) is zero in this calculation. Then we increase the applied Lorentz force linearly with time and calculate $\hat{v}_x$ for each increment. At each increment, we calculate 1.0×10^5 MD steps. Then, we discard the values of first 5×10^4 MD steps and average those of the remaining 5×10^4 MD steps. The average vortex velocity and the Lorentz force are related to macroscopically

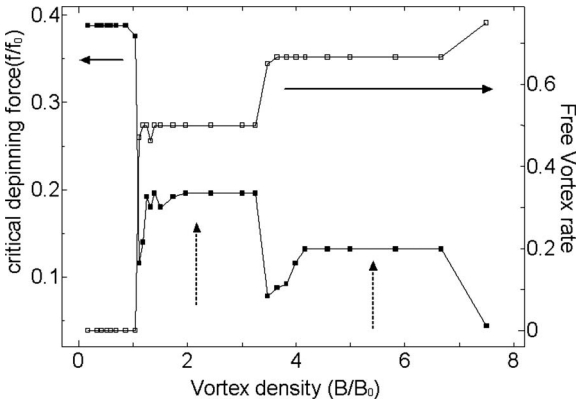

FIG. 1. Critical depinning force (f_{cr}) and FVR as a function of vortex density curve for $f_{\mathrm{tb}}=f_0$. Both of them change in staircase pattern. Steps indicated by upward arrow correspond to broad matching peaks.

measured voltage and current respectively. We define the critical depinning force f_{cr} as the force when $\hat{v}_x$ reaches the value of 0.03 times of linear response in an unpinned ideal sample ($\hat{v}_x=f_L$). This criterion was used in previous reports and thought to be valid.[31,38] The f_{cr} represents the transition point between vortex pinned state and moving state and is related to the critical current density.

After reaching high Lorentz force where vortices form moving vortex lattices, we decrease Lorentz force down to zero and check the final vortex positions. In most of our calculations, the final positions are close enough to their initial ones but differ substantially from initial ones in some cases. In such cases, f_{cr} changes greatly in the second calculation of V-I curve using the final positions as new initial positions. The V-I curve converged after we repeated calculations several times, and we determined f_{cr} from the converged curves.

III. RESULTS

In Fig. 1, we show f_{cr} and free vortex rate (FVR) as a function of vortex density for strong pinning case ($f_{\mathrm{tb}}=f_0$). In this case, maximum pinning force of TB f_p is estimated as $0.38\ f_0$ from Eq. (3). The value of FVR represents the ratio of depinned vortices to all vortices below f_{cr}. From Fig. 1, we can see steplike changes of f_{cr} and FVR. We found that this behavior corresponds to drastic change of vortex configurations. Figures 2(a) and 2(b) show vortex positions (black circles) and TBs (shaded line regions) at $0.69B_0$ and $1.04B_0$, respectively. In this manner, all vortices are pinned by TBs and form an ordered lattice along the TBs up to $\sim B_0$. Thus FVR equals zero, and f_{cr} equals f_p. In the region from $1.3B_0$ to $3.3B_0$, vortices again form an ordered lattice but one vortex line appears along the y axis between neighboring TBs, as shown in Figs. 2(c) and 2(d). In these configurations, half of vortices are pinned, i.e., FVR equals 1/2, so that f_{cr} equals $1/2f_p$. Similarly, in the region from $4.2B_0$ to $6.7B_0$, vortices form an ordered lattice with two vortex lines appearing between neighboring TBs, as shown in Figs. 2(e) and 2(f). Here, FVR equals 2/3, so that f_{cr} equals $1/3f_p$. Mean-

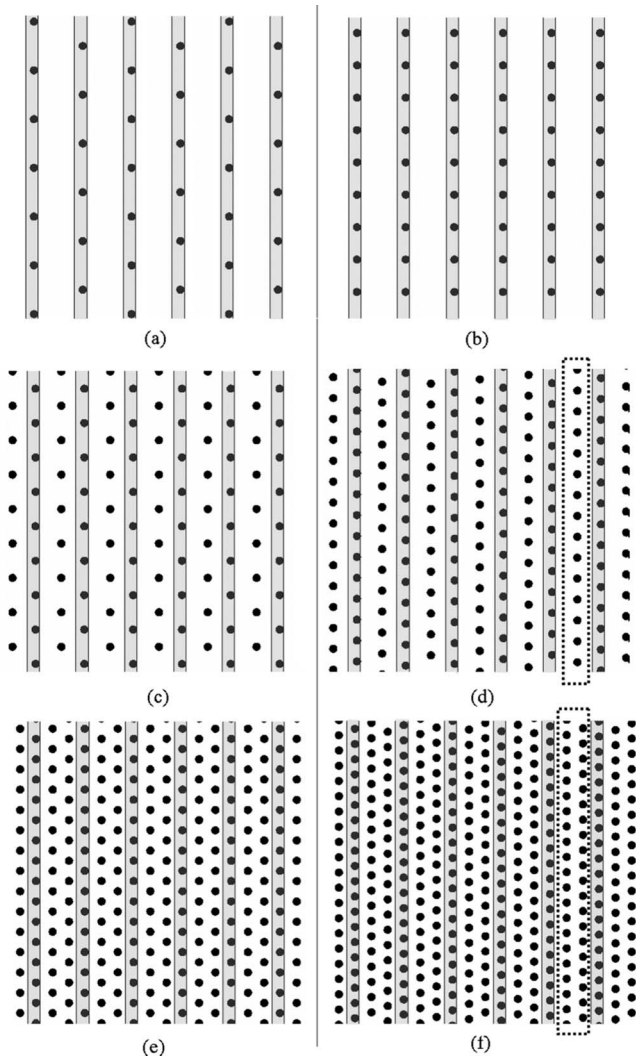

FIG. 2. The static vortex positions below f_{cr} (black circles) and TBs arrangement (shaded regions) at (a) $0.69B_0$, (b) $1.04B_0$, (c) $2.43B_0$, (d) $3.24B_0$, (e) $5.00B_0$, and (f) $6.66B_0$.

while, around $1.2B_0$, f_{cr} are lower than $1/2f_p$, even though FVR are 1/2. In this region vortices have some spatial order, but their configurations do not fit in the periodic structure of TBs as seen in the case of $1.11B_0$ shown in Fig. 3(a). In consequence, pinning efficiency decreases and f_{cr} becomes

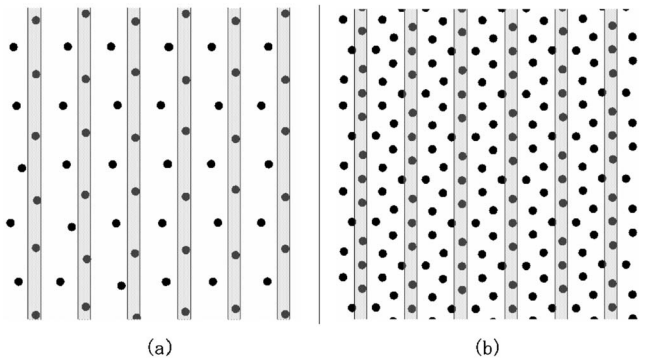

FIG. 3. The static vortex positions below f_{cr} and TBs arrangement at (a) $1.11B_0$ and (b) $3.65B_0$.

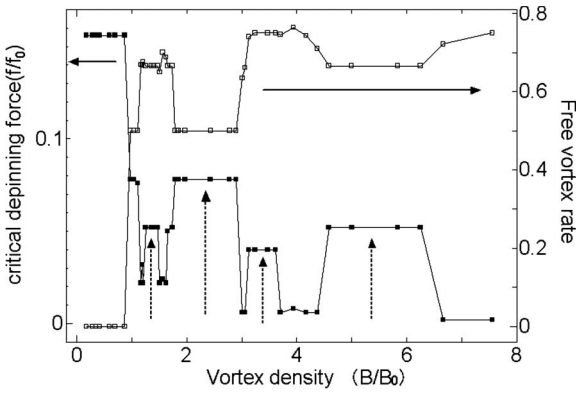

FIG. 4. Critical depinning force (f_{cr}) and FVR as a function of vortex density curve for $f_{tb}=0.4\ f_0$. Steps indicated by upward-arrow correspond to broad matching peaks.

lower than $1/2\ f_p$. In the same way, around $3.5B_0$ vortices do not form an ordered lattice that fits in the periodic structure of TBs as seen in Fig. 3(b), and f_{cr} becomes lower than $1/3f_p$.

In Fig. 4, we plot f_{cr} and FVR as a function of vortex density for weak pinning case ($f_{tb}=0.4f_0$). In this case, f_p equals $0.15f_0$. The most significant feature seen in Fig. 4 is that additional steps appear around $1.4B_0$ and $3.5B_0$ compared with the case of $f_{tb}=f_0$. Furthermore, additional terraces appear around $1.1B_0$ and $1.8B_0$. In the step region around $1.4B_0$, vortices form an ordered triangle lattice whose height is equal to two thirds of twin spacing [Fig. 5(b) for $1.35B_0$], that is, FVR is 2/3 and f_{cr} equals $1/3f_p$. In contrast, in dip regions next to the step ones around $1.4B_0$, vortices do not form an ordered lattice that fits in the periodic structure of TBs and f_{cr} becomes lower than $1/3f_p$ [see Figs. 5(a) and 5(c) for $1.19B_0$ and $1.56\ B_0$]. A similar situation occurs around $3.5B_0$ [see Figs. 6(a)–6(c) for $3.06B_0$, $3.47B_0$, and $3.70B_0$]. In this case a triangle lattice appears whose base length is equal to half of twin spacing. In the terrace region, other types of vortex lattices appear whose base length is equal to twin spacing for $1.1B_0$ and two-third of twin spacing for $1.8B_0$.

In Fig. 7, we show the average vortex velocity $\hat{v}_x$ versus the Lorentz force f_L at $1.09B_0$, $1.51B_0$, and $3.47B_0$ in strong pinning case. At $1.51B_0$ and $3.47B_0$, $\hat{v}_x-f_L$ curves show single jump. This single jump means that all the vortices start to move simultaneously at this point. Meanwhile, at $1.09B_0$, we observe multiple jumps. The curves show first small jump at $f_L=0.1f_0$, which means vortices start to flow and final jump at $f_L=0.32f_0$. In both the region from $f_L=0.1f_0$ to $0.32f_0$ and that of $f_L>0.32f_0$, $\hat{v}_x$ varies linearly with f_L, but the $\hat{v}_x-f_L$ slope in the former is much smaller than the slope in the latter ($\hat{v}_x \simeq f_L$). In the former region, a portion of vortices flow while the other portions remain pinned, and this type of flow corresponds to the "plastic flow." In our simulation, in both strong and weak pinning cases, the multiple jumps and plastic flow are observed only in some dip regions, and the $\hat{v}_x-f_L$ curves in other cases always have single jump. The value of f_{cr} corresponds to the position of first jump of these curves.

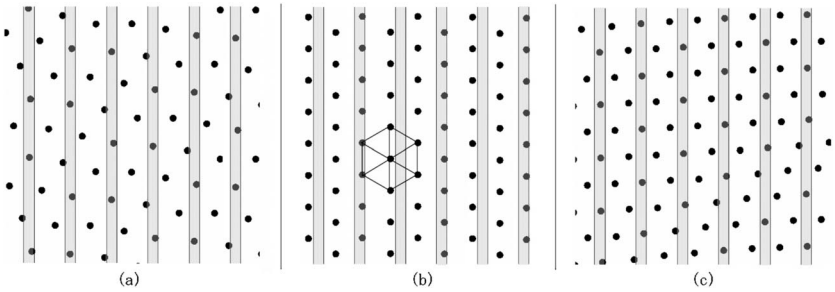

FIG. 5. The vortex positions and TBs arrangements at (a) $1.19B_0$, (b) $1.35B_0$, and (c) $1.56B_0$.

IV. DISCUSSION

Here, we analyze these results from the viewpoint of matching effect. For thin-film superconductors with periodic arrays of columnar defects, some groups reported that matching effects appear as sharp peaks in the f_{cr} vs vortex density curve.[29–31] In the present study, f_{cr} go up and down with increasing the vortex density, and f_{cr} steps appear. At the steps indicated by arrows in Figs. 1 and 4, the pinning efficiency has increased due to the commensuration between the vortex lattice and the arrangement of TBs. Therefore, we can regard such steps as matching peaks, though their "broad" width is different from the "sharp" matching peaks reported in the columnar pinning case. This difference can be explained from the capacity of the pinning center to trap vortices. In general, one columnar pinning can trap only one vortex. Hence vortex lattices fitting in periodic pinning arrays are formed only at specific vortex densities. Meanwhile, one TB can trap multiple vortices in its plane so that vortices can form commensurate lattice flexibly as seen in the configuration change from Fig. 2(c) to Fig. 2(d). As a result, the width of matching peak in the TB case is wider than that of the columnar pinning case. It should be noted that similar broad matching effect has been reported in the superconductor with quasiperiodic pinning arrays.[1–5] In this case, the broad matching peaks come from the proliferation of matching peaks associated with the different kinds of local structures found in quasiperiodic pinning arrays. Anyway, these broad matching peaks could be useful for practical applications demanding high J_c's over a wide range of magnetic fields.

Let us now consider the different vortex configurations between strong and weak pinning cases. This difference can be understood from the relation between pinning energy and vortex-vortex interaction energy. In general, vortices tend to form a regular triangle lattice due to the repulsive interacting force. In the strong pinning case, stabilization caused by pinning has larger effect than that caused by lattice formation. Therefore, vortices can form structures, which deviate from regular triangle lattice but have large number of pinned vortices, as shown in Fig. 2. On the other hand, in the weak pinning case, stabilization caused by pinning has smaller effect than that caused by lattice formation. Thus vortices tend to form structures, which are close to regular triangle lattice, as shown in Figs. 5(b) and 6(b). These configuration changes lead to the appearance of the additional matching peaks. It should be noted that other possible matching lattices do not appear. For example, the vortex lattice shown in Fig. 8, whose height is equal to three fifth of twin spacing, is suitable configuration around $1.7B_0$ from the viewpoint of lattice constant. In this structure, however, FVR becomes 4/5 and stabilization by pinning becomes smaller than the one in the structure shown in Fig. 5(c) where FVR nearly equals 2/3. Such decrease in the pinning energy suppresses the appearance of the vortex lattice where FVR is large. Of course, this mechanism for the appearance of lattice structure depends on the pinning strength, and the matching lattice shown in Fig. 8 can appear in weaker pinning cases.

Finally, we compare our results with previous works on similar vortex systems. The 2D vortex configuration and matching effect in the presence of trigonometric potential has been discussed theoretically.[33–35] In these studies, triangular matching configurations are given by

$$B_{n_1,n_2} = \frac{\sqrt{3}}{2}\frac{\Phi_0}{\lambda_g^2}(n_1^2 + n_2^2 + n_1 n_2)^{-1}, \tag{4}$$

where λ_g is the wavelength of potential modulation. In Ref. 35, the authors predicted the presence of locked phase where vortices form triangle lattices fitting in periodic pinning structure and a transition from the locked phase to "unlocked phase" where vortices form lattices not fitting in periodic pinning structure and having 1D periodic sequence of domain walls. However, they analyzed only the vortex configurations that satisfy $d \geq \lambda_g$. On the other hand, we have also analyzed vortex configurations in the region where $d < \lambda_g$ and observed commensurate lattices and incommensurate

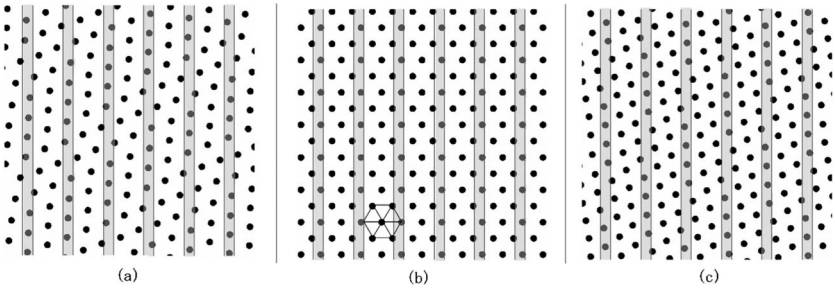

FIG. 6. The vortex positions and TB arrangements at (a) $3.06B_0$, (b) $3.47B_0$, and (c) $3.70\ B_0$.

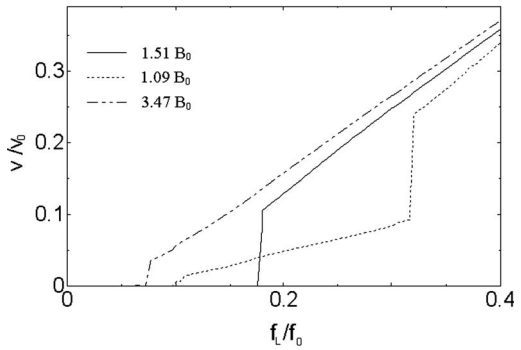

FIG. 7. Average vortex velocity $\hat{v}_x$ versus Lorentz force f_L curves at $1.09B_0$, $1.51B_0$, and $3.47B_0$ in strong pinning case.

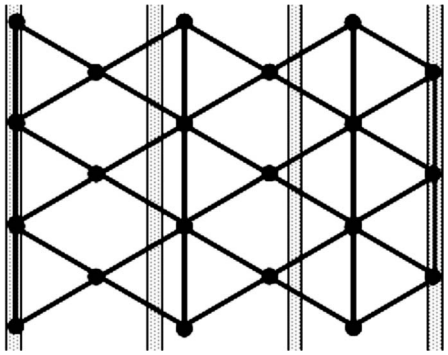

FIG. 8. Schematic sketch of regular triangle lattice whose height is equal to 3/5 of twin spacing.

lattices, which correspond to locked phase and unlocked phase, respectively. As discussed above, the transitions between the commensurate and incommensurate lattices lead to the appearance of broad matching peaks. In addition, even in the case of $d \geq \lambda_g (\sim 0.6B_0)$, we observe a behavior a little different from the ones in Ref. 35. Although we observe the matching triangular lattice at $B_{1,0}, B_{1,1}$ as reported in Ref. 35 (we do not perform calculation in lower vortex density region where $B \leq B_{1,1}$), the unlocked phase does not appear while it does in Ref. 35. This is because in our calculation the stabilization by pinning is larger than that by lattice formation even in the weak pinning case, while pinning strength is set to be smaller than the lattice stiffness in Ref. 35.

The matching effect has also been observed experimentally in the superconductor whose thickness has 1D periodic modulation.[32] In this study, the authors have reported broad matching effect around $\Phi_0/(2\lambda_g)^2$, Φ_0/λ_g^2, $\Phi_0/(\lambda_g/2)^2$, and $\Phi_0/(\lambda_g/3)^2$. The positions of these peaks correspond to $0.15B_0$, $0.60B_0$, $2.40B_0$, and $5.42B_0$ in our results. Additionally, they have reported disappearance of matching effect at low temperature. They explained this phenomenon by weakening of vortex interaction coming from the decrease in the penetration depth. This phenomenon is consistent with the suppression of matching peaks in our results. In our calculation, we observe matching peaks around $2.4B_0$ and $5.4B_0$, while we do not observe any peaks up to $\sim B_0$ for the reasons mentioned above. What has to be noticed is that the peaks seen around $1.4B_0$ and $3.5B_0$ in the weak pinning case of our calculation have not been observed in Ref. 32. As discussed above, the appearance of these peaks are caused by the formation of vortex lattices which fit in underlying periodic pinning arrays. Thus, the appearance of these peaks is sensitive to lattice formation and could be easily disturbed by little deviation of the pinning arrangements in real samples from ideally periodic one or lattice disorder coming from thermal fluctuation. Moreover, there is a possibility that the difference of the ratio of pinning potential width to λ_g causes the difference of matching peaks. This is because the value of FVR, which is strongly related to the value of f_{cr}, depends on this ratio. For example, FVR is always zero when this ratio equals 1. Furthermore, the vortex structure would also vary with this ratio. However, since this ratio has not been given in Ref. 32, we cannot tell whether the difference of this ratio is also responsible for the discrepancy between the feature of matching peaks between their and our results.

V. CONCLUSIONS

We have investigated dynamics of vortices interacting with unidirectional TBs using molecular-dynamics simulation. First we have found that the critical depinning force (f_{cr}) as a function of vortex density shows a steplike pattern which depends on the pinning strength. This behavior corresponds to drastic change of vortex configurations, which reflects the pinning characteristic of TBs. Next we have found broad f_{cr} peaks coming from the matching effects and also found that the appearance of some of these peaks are suppressed in the strong pinning case.

In our calculation, we ignore several effects such as point defects and fluctuation of vortex lines for simplicity. However, our results provide us with basic understanding of the pinning property of TB and may be helpful in interpreting experimental results. The results of our study are consistent with the experimental results in the superconducting films whose thickness is periodically modulated in one direction.[32] We can expect that our results are useful for other types of planar pinning systems such as laminar structure in Bi2Sr2CaCu2O8+y sample.[39] Furthermore, our study is correlated with other types of many particle problems, e.g., colloidal particles on periodic 1D substrates.[40]

ACKNOWLEDGMENTS

We wish to thank X. Hu and K. Matsushita (National Institute for Materials Science) for valuable advice and C. Reichhardt (Los Alamos National Laboratory) for useful discussion.

*asai@cello.t.u-tokyo.ac.jp

[1] A. V. Silhanek, W. Gillijns, V. V. Moshchalkov, B. Y. Zhu, J. Moonens, and L. H. A. Leunissen, Appl. Phys. Lett. **89**, 152507 (2006).
[2] M. Kemmler, C. Gürlich, A. Sterck, H. Pöhler, M. Neuhaus, M. Siegel, R. Kleiner, and D. Koelle, Phys. Rev. Lett. **97**, 147003 (2006).
[3] J. E. Villegas, M. I. Montero, C.-P. Li, and I. K. Schuller, Phys. Rev. Lett. **97**, 027002 (2006).
[4] V. Misko, S. Savel'ev, and F. Nori, Phys. Rev. Lett. **95**, 177007 (2005).
[5] V. R. Misko, S. Savel'ev, and F. Nori, Phys. Rev. B **74**, 024522 (2006).
[6] A. Goyal, S. Kang, K. J. Leonald, P. M. Martin, A. A. Gapud, M. Varela, M. Paranthaman, A. O. Ijaduola, E. D. Specht, J. R. Thompson, D. K. Christen, S. J. Pennycook, and F. A. List, Supercond. Sci. Technol. **18**, 1533 (2005).
[7] L. Shlyk, G. Krabbes, G. Fuchs, and K. Nenkov, Appl. Phys. Lett. **86**, 092503 (2005).
[8] S. R. Foltyn, L. Civale, J. L. MacManus-Driscoll, Q. X. Jia, B. Maiorov, H. Wang, and M. Maley, Nat. Mater. **6**, 631 (2007).
[9] J. E. Villegas, S. Savel'ev, F. Nori, E. M. Gonzalez, J. V. Anguita, R. Garcia, and J. L. Vicent, Science **302**, 1188 (2003).
[10] J. Van de Vondel, C. C. de Souza Silva, B. Y. Zhu, M. Morelle, and V. V. Moshchalkov, Phys. Rev. Lett. **94**, 057003 (2005).
[11] D. S. Fisher, M. P. A. Fisher, and D. A. Huse, Phys. Rev. B **43**, 130 (1991).
[12] D. R. Nelson and V. M. Vinokur, Phys. Rev. B **48**, 13060 (1993).
[13] Y. Nonomura and X. Hu, Physica C **408-410**, 529 (2004).
[14] R. Sugano, T. Onogi, K. Hirata, and M. Tachiki, Physica C **388-389**, 637 (2003).
[15] H. Beidenkopf, N. Avraham, Y. Myasoedov, H. Shtrikman, E. Zeldov, B. Rosenstein, E. H. Brandt, and T. Tamegai, Phys. Rev. Lett. **95**, 257004 (2005).
[16] G. Blatter, M. V. Feigel'man, V. B. Geshkenbein, A. I. Larkin, and V. M. Vinokur, Rev. Mod. Phys. **66**, 1125 (1994).
[17] M. Oussena, P. A. J. de Groot, S. J. Porter, R. Gagnon, and L. Taillefer, Phys. Rev. B **51**, 1389 (1995).
[18] W. K. Kwok, J. A. Fendrich, V. M. Vinokur, A. E. Koshelev, and G. W. Crabtree, Phys. Rev. Lett. **76**, 4596 (1996).
[19] Z. W. Lin, G. D. Gu, A. S. Mahmoud, and G. J. Russell, Physica C **349**, 95 (2001).
[20] J. Groth, C. Reichhardt, C. J. Olson, S. B. Field, and F. Nori, Phys. Rev. Lett. **77**, 3625 (1996).
[21] B. Y. Zhu, J. Dong, D. Y. Xing, and Z. D. Wang, Phys. Rev. B **57**, 5075 (1998).
[22] C. Reichhardt, C. J. Olson, and F. Nori, Phys. Rev. B **61**, 3665 (2000).
[23] Y. Enomoto and T. Mitsuda, Physica C **367**, 60 (2002).
[24] G. W. Crabtree, D. O. Gunter, H. G. Kaper, A. E. Koshelev, G. K. Leaf, and V. M. Vinokur, Phys. Rev. B **61**, 1446 (2000).
[25] T. Naito, H. Iwasaki, T. Nishizaki, and N. Kobayashi, Phys. Rev. B **70**, 014515 (2004).
[26] O. Jongprateep and S.-W. Chan, IEEE Trans. Appl. Supercond. **13**, 3502 (2003).
[27] L. Mei, V. S. Boyko, and S.-W. Chan, Physica C **439**, 78 (2006).
[28] L. Shlyk, G. Krabbes, G. Fuchs, C. Mickel, B. Rellinghaus, and K. Nenkov, Appl. Phys. Lett. **88**, 062509 (2006).
[29] V. V. Metlushko, M. Baert, R. Jonckheere, V. V. Moshchalkov, and Y. Bruynseraede, Solid State Commun. **91**, 331 (1994).
[30] V. Metlushko, U. Welp, G. W. Crabtree, R. Osgood, S. D. Bader, L. E. DeLong, Z. Zhang, S. R. J. Brueck, B. Ilic, K. Chung, and P. J. Hesketh, Phys. Rev. B **60**, R12585 (1999).
[31] C. Reichhardt and N. Grønbech-Jensen, Phys. Rev. B **63**, 054510 (2001).
[32] O. Daldini, P. Martinoli, J. L. Olsen, and G. Berner, Phys. Rev. Lett. **32**, 218 (1974).
[33] P. Martinoli, Phys. Rev. B **17**, 1175 (1978).
[34] P. Martinoli, H. Beck, M. Nsabimana, and G.-A. Racine, Physica B & C **107B**, 455 (1981).
[35] P. Martinoli, M. Nsabimana, G.-A. Racine, and H. Beck, Helv. Phys. Acta **55**, 655 (1982).
[36] M. Kulic and F. S. Rys, J. Low Temp. Phys. **76**, 167 (1989).
[37] M. I. J. Probert and A. I. M. Rae, Phys. Rev. Lett. **75**, 1835 (1995).
[38] I. M. Obaidat, U. A. L. Khawaja, and M. Benkraouda, Supercond. Sci. Technol. **18**, 1380 (2005).
[39] K. Itaka, H. Taoka, S. Ooi, T. Shibauchi, and T. Tamegai, Phys. Rev. B **60**, R9951 (1999).
[40] C. Reichhardt and C. J. Olson Reichhardt, Phys. Rev. E **72**, 032401 (2005).